Correlation between Grafting Density and Confined Crystallization Behavior of Polyethylene Glycol Grafted to Silica

Xiangning Wen,[a,b] Yunlan Su,[a,b],* Yudan Shui,[a] Weiwei Zhao,[a]

Alejandro J. Müller,[c,d] * Dujin Wang[a,b]

[a] Key Laboratory of Engineering Plastics, CAS Research/Education Center for Excellence in Molecular Sciences, Institute of Chemistry, Chinese Academy of Sciences, Beijing 100190, China

[b] University of Chinese Academy of Sciences, Beijing 100049, China

[c] POLYMAT and Polymer Science and Technology Department, Faculty of Chemistry, University of the Basque Country UPV/EHU, Paseo Manuel de Lardizabal 3, 20018 Donostia-San Sebastián, Spain

[d] IKERBASQUE, Basque Foundation for Science, Bilbao, Spain

ABSTRACT

The interfacial interactions of polymer-nanoparticles have dramatical effects on the crystallization behavior of grafted polymers. In this study, methoxy polyethylene glycol (MPEG) (molecular weights 750, 2000 and 4000 g mol^{-1}) was grafted onto amino-modified nanosized silica (SiO_2-NH_2) by the “grafting to” method. The effects of the grafting density and molecular weight on the confined crystallization of grafted MPEG (MPEG-*g*-SiO_2) were systematically investigated by differential scanning calorimetry (DSC), thermogravimetric analysis (TGA) and wide-angle X-ray scattering (WAXS). It was found that confinement effects are stronger when lower molecular weights of grafted MPEG are employed. These grafted MPEG chains are more difficult to stretch out on SiO_2-NH_2 surfaces than when they are free in the bulk polymer. Both crystallization temperature (T_c) and crystallinity of grafted MPEG chains decrease with reductions of grafting density. Additionally, covalent bonding effects and interfacial interaction confinement effects are strengthened by the decrease in grafting density, leading to an increase in decomposition temperature and to the disappearance of the self-nucleation *Domain* (i.e., *Domain II*), when self-nucleation experiments are performed by DSC. Overall isothermal crystallization kinetics was studied by DSC and the results were analyzed with the Avrami equation. An Avrami index of $n \approx 3$ was obtained for neat MPEG (indicating that instantaneous spherulites are formed). However, in the case of MPEG-*g*-SiO_2 with the lowest grafting density, the Avrami index of (n) was less than 1 (first order kinetics or lower), indicating that nucleation is the determining factor of the overall crystallization kinetics, a signature

for confined crystallization. At the same time, the crystallization from the melt for this MPEG-*g*-SiO_2 with the lowest grafting density occurs at $T_c \approx$-30 ºC, a temperature close to the glass transition temperature (T_g) of MPEG, indicating that this confined MPEG crystallizes from homogeneous nuclei.

Keywords: confined crystallization; Stöber silica; nanoparticles; poly (ethylene glycol)

INTRODUCTION

The inclusion of nanoparticles can enhance the properties of polymeric materials and contribute to the continuous development of multi-functional composite materials.[1] With superior physical and chemical properties, polymer nanocomposites (PNCs) have valuable potential applications in optoelectronic materials, microelectronic devices, biosensors and molecular recognition.[2-3] The performance of polymer nanocomposites is crucially related to the intrinsic properties of the parent materials, as well as nanoparticles size, dispersion and interfacial compatibility. PNCs can even display synergistic behavior.[4-7] The dispersion state of the nanoparticles in the polymeric matrix is an essential factor for obtaining PNCs enhanced properties. The modification of nanoparticles by chemical grafting, usually leads to an efficient control of the dispersion of the nanoparticles in the matrix.[8-9]

A considerable amount of research has been devoted to study the special properties of polymer-grafted nanoparticles (PGNPs), such as the compatibility with the polymer matrix,[10] interfacial interactions,[11] conformation and glass transitions[12] of grafted chains. Previous works found that the grafting density, segmental length and matrix molecular weight have significant influence on the compatibility of the composites.[13] In the case of polymer-*g*-SiO_2 nanocomposites, it has been reported that the occupied area of the grafted chains on SiO_2 exhibits an increasing trend with the decrease of grafting density, thereby displaying stronger interfacial effects.[14]

When polymer chains are in confined environments (such as inside AAO nanopores, or within block copolymers strongly segregated matrices), they can

experience changes in their overall isothermal crystallization kinetics and in crystal orientation. Crystallization kinetics can change from the typical sigmoidal type to that of a first order crystallization kinetics (as a result of changes in their nucleation mechanism from heterogeneous to homogeneous).[15-20]

Tethering polymer chains onto nanoparticles provides an excellent model to understand the confined crystallization mechanism of grafted polymers, which is determined by nanoparticle size, molecular weight and grafting density.[21-22] Zhou et al.[23] have reported that lamellar thicknesses of the crystallites formed by grafted chains are smaller as the molecular weight decreases. Jana and Cho[24] also discussed the molecular weight impact on the crystallization behavior of polymer brushes grafted on carbon nanotubes. They found that the crystallization ability of grafted chains increased, as the molecular weight of the grafted chains was higher.

According to theoretical investigations, the crystallization ability of grafted chains increases at higher grafting density[21] and faster crystallization rates can be obtained[22]. Moreover, the grafted chains tend to adopt a more extended conformation with increases in grafting density until at high grafting ratio, the dominant conformation is that of the so called "tails" conformation.[25-26] Kim and Archer[21] grafted poly (ethylene glycol) (PEG) onto SiO_2 nanoparticles and found that PEG chains exhibit more *trans* conformations at higher grafting density and more *gauche* conformations at lower grafting density.

However, in these previous studies, the grafting density varied when the molecular weight of the grafted chains increased and the effect of the two structural

factors had not been explored independently so far. Less attention has been paid to the confined crystallization behavior imposed by grafting density and molecular weight of the grafted polymers on SiO_2 surface, whereas these effects have been extensively reported for polymers confined in other systems, such as carbon nanotubes[24] and block copolymers with grafted brushes.[27-28]

Poly(ethylene oxide) is an attractive semicrystalline polymer for fundamental research[29-30] and its silica nanocomposites can increase ion conductivity for applications in solid-state lithium batteries materials[31-32].

The main goal of this paper is to systematically study the effect of changing grafting density, molecular weight and silica content on the crystallization behavior of grafted methoxy polyethylene glycol (MPEG) chains. We have used the "grafting to" method,[33-34] where MPEG chains (with molecular weights of 750, 2000 and 4000 g mol^{-1}) were grafted onto amino-modified nanosilica in a mixed solvent. We have chosen three different molecular weights of MPEG and the grafting density has been varied in a wide range. The results demonstrate that grafting density plays a crucial role in the nucleation and crystallization of grafted MPEG chains. At the lowest grafting density, confinement effects lead to homogeneous nucleation and to approximately first order crystallization kinetics of MPEG chains.

EXPERIMENTAL

Materials

Methoxy polyethylene glycols (M_n =750 g·mol^{-1}, PDI =1.07; M_n = 2000 g·mol^{-1},

PDI =1.06; M_n = 4000 g·mol^{-1}, PDI =1.09; PDI was characterized by GPC presented in Fig. S1.), MPEG, were purchased from TCI Co., Tokyo, Japan. Monodispersed spherical silica nanoparticles with an average particle size of 50 nm were obtained by the Stöber method.[35] N-(2-aminoethy)-3-aminopropylmethyldimethoxysilane (ADMS) was purchased from Alfa Aesar Co., Shanghai, China.

Sample Preparation

The preparation of MPEG-*g*-SiO_2 has been previously reported by Shui et al. [36] In this work, we used the same method, the well-defined siloxane structure (SiO_2-NH_2) was obtained with ADMS by a silanization coupling reaction. Then, epoxide terminated MPEG (molecular weight 750, 2000 and 4000 g mol^{-1}) (MPEG-EO) was coupled to the amino-modified silica (SiO_2-NH_2) by the reaction of their terminal groups in a mixed solvent (*n*-decane/toluene). Grafting density was controlled by the solvent ratio. SiO_2-NH_2 grafted with different molecular weights of MPEG was denoted as MPEG*x*-*g*-SiO_2, where *x* represents the molecular weight of MPEG.

Characterization

Transmission Electron Microscope

The dispersion state of grafted SiO_2 was examined by a HT-7700 transmission electron microscope (TEM) with an operating voltage of 100 KV. The sample was dispersed in ethanol and ultrasound for 5 min then deposited on the carbon-coated copper grid.

Small Angle X-ray Diffraction

The small angle X-ray diffraction (SAXS) measurements were carried out at the

beamline BL16B1 at Shanghai Synchrotron Radiation Facility (SSRF) at 90 °C. In order to eliminate the signal of grafted PEO, the temperature is set above the T_m of PEO. The wavelength of the radiation source was λ = 1.24 Å. The sample to detector distance was 2105 mm. 2D SAXS patterns were transformed into 1D intensity profiles by using the Fit2D software.

Thermogravimetric Analysis

The grafting density of MPEG was calculated by thermogravimetric analysis (PE8000, USA). Samples of 2-3 mg were heated from 50 to 100 ºC at a rate of 40 ºC/min and held for 2 min at 100 ºC to remove physically adsorbed water, then heated from 100 to 850 ºC at a rate of 20 ºC/min.

Differential Scanning Calorimetry

A TA-Q2000 DSC apparatus was employed to study the non-isothermal crystallization and melting behavior of grafted MPEG chains. The equipment was calibrated with indium and ultra-pure nitrogen was used as purge gas. The samples (3-5 mg) were encapsulated in Aluminium pans. Firstly, the samples were heated to 100 ºC and held at that temperature for 3 min to erase their crystalline history. Secondly, they were cooled to -80 ºC, and finally, reheated to 100 ºC. All tests were performed at a cooling and heating rate of 10 ºC/min. The peak melting (T_m) and crystallization (T_c) temperatures were recorded. The crystallinity (X_c) was calculated by the following equation:

$$X_C(\%) = \frac{\Delta H_m(J/g)}{\Delta H_m^0(J/g)} * 100\% \quad (1)$$

where ΔH_m is melting enthalpy normalized by the weight of grafted chains and ΔH_m^0 is the melting enthalpy of 100% crystalline PEO[37] with a value of 205 J/g.

For the isothermal crystallization process, different methods were adopted to analyse the crystallization kinetics of grafted MPEG. In the case of neat MPEG, the isothermal crystallization behavior was performed by continuous monitoring of the heat evolved during crystallization as a function of time in the DSC.[38] The samples were heated to 100 ºC for 3 minutes to erase thermal history, then they were cooled at 60 ºC /min to a T_c value where the isothermal DSC experiment was performed. The isothermal DSC tests were performed in a Perkin-Elmer Diamond DSC.

In the case of the grafted polymer samples, because of the confinement effects exerted by the large amounts of SiO_2-NH_2, the crystallization rate was so slow that the amount of heat evolved during crystallization per unit time was beyond the resolution of the instrument. Therefore, we used isothermal step crystallization (ISC) experiments[39-40] to investigate the crystallization mechanism of grafted chains. They were performed on the TA-Q200 DSC instrument. The isothermal step crystallization method applied is described below:

(a) The specimen was heated to 100 ºC for 3 min to erase thermal history.

(b) Fast cooling from 100 ºC to a chosen crystallization temperature (T_c) at 60 ºC/min

(c) Isothermal step for a certain crystallization time (t_c) at T_c.

(d) Heating from T_c to 100 ºC at 10 ºC/min. The heat of fusion during this DSC heating scan is assumed to correspond to the crystallization enthalpy at T_c for a given t_c.

(e) Steps a through d were repeated at the same T_c, but at increasing t_c values until the melting enthalpy did not change anymore with t_c.

(f) Finally, the whole procedure was repeated at different T_c values

The obtained data were analyzed with the Avrami equation[38]**:**

$$1\text{-}V_c(t\text{-}t_0) = \exp(\text{-}K(t\text{-}t_0)^n \quad (2)$$

where n is the Avrami index, K is the rate constant of the crystallization process, t_0 is the induction time and V_c is the relative volume fraction which can be obtained from the following equation:

$$V_c(t-t_0) = \frac{w_c}{w_c + \frac{\rho_c}{\rho_a}(1-w_c)} \quad (3)$$

Where, ρ_c= 1.23 g/cm^3 and ρ_a =1.12 g/cm^3 correspond to the crystalline and amorphous densities of PEO, respectively.[41] w_c is the relative mass crystalline fraction calculated by the following equation:

$$W_c = \frac{\Delta H(t)}{\Delta H_{total}} \quad (4)$$

Where ΔH_{total} is the final melting enthalpy (after saturation of the crystallization) and ΔH (t) indicates the melting enthalpy at a specified t_c. The experimental results are fitted by the Avrami equation in the primary crystallization range of 5 % to 35 %, as the secondary crystallization frequently causes significant deviations from the fit.[38]

In order to study the effect of high concentrations of silica on nucleation, self-nucleation experiments have been performed based on the protocol designed by Fillon et al.[42] The self-nucleation (SN) experiments [42-43] were performed in the TA-Q2000 DSC apparatus. The samples were heated to 100 ºC employing a heating rate of 10 ºC/min and were held at that temperature for 3 min to erase thermal history. Then, they were cooled to -60 ºC at 10 ºC/min in order to give the sample a standard thermal history. After 3 min stabilization time at -60 ºC, the samples were heated (also

at 10 ºC/min) up to a chosen self-nucleation temperature (T_s) and held at that temperature for 5 min. Depending on the value of T_s, the sample could completely melt (*Domain I* or melting *Domain*), self-nucleate (*Domain II* or exclusive self-nucleation *Domain*, where the sample is self-nucleated and experiments no annealing), or self-nucleate and anneal (*Domain III* or self-nucleation and annealing *Domain*, where the sample is partially molten and the unmolten crystals are annealed). The samples were cooled from T_s at 10 ºC/min down to -60 ºC and during this cooling scan, the effects of the thermal treatment at T_s can be appreciated. Finally, the samples were heated at 10 ºC/min. In this final heating run, the effects of crystallization, self-nucleation and annealing (if present) could be ascertained.

RESULTS AND DISCUSSION

The Dispersion State of MPEG-*g*-SiO_2

The physicochemical properties of PNCs are influenced by the dispersion state of nanoparticles. A combination of TEM and SAXS is typically used to evaluate the dispersion state of the nanoparticles.[44-45] TEM provided us with images of the dispersion state of grafted SiO_2 in the limited microscopic areas that were observed. SAXS enabled us to assess the dispersion over the scattering volume in larger sample sizes. The strong upturn in the low q region of SAXS curves represents phase-separated or aggregated structures with dimensions outside the probe length in SAXS measurements,[46] whereas the plateau in low q region represents a well-dispersed system.[44]

Figures 1a-c and e-h show TEM micrographs of MPEG-*g*-SiO_2 samples with

different molecular weights at highest σ, in which σ (chain/nm^2) is the grafting density[47]. The MPEG grafted SiO_2 and bare SiO_2 are both near-spherical in shape (the individual grafted SiO_2 with spherical shape is clearly shown in Figure 1f). No large aggregates were detected by TEM before or after MPEG is grafted to the silica surface.

Figure 1i shows the SAXS curves of the three molecular weights MPEG-*g*-SiO_2, in which *I(q)* in the low *q* region (from 0.008 Å^{-1} to 0.01 Å^{-1}) shows a plateau for these three grafted nanoparticles. This indicates no scattering from large-scale aggregates which agrees well with TEM results.

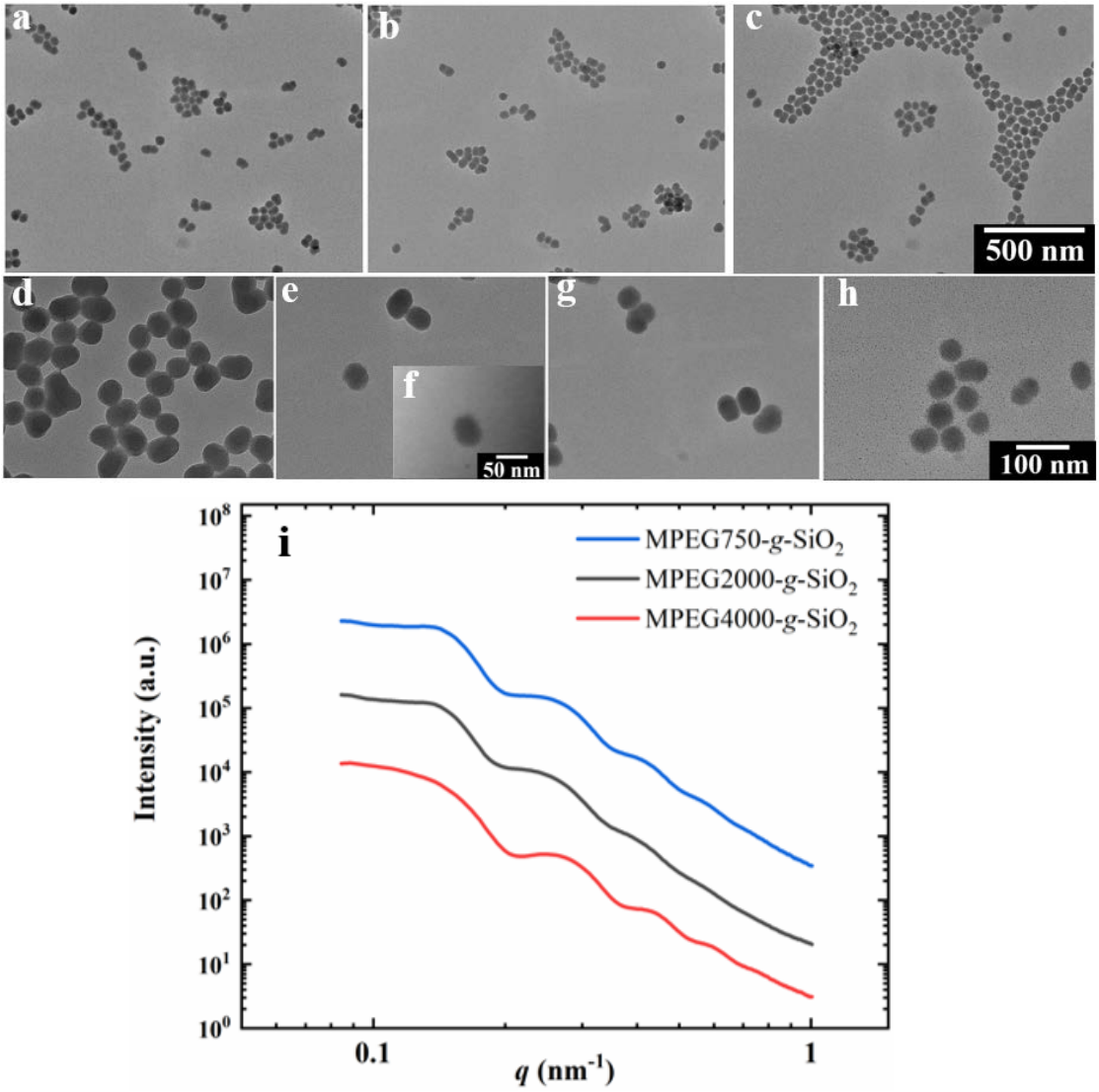

Figure 1. *TEM images of grafted SiO_2 (a) MPEG750-g-SiO_2; (b) MPEG2000-g-SiO_2; (c)MPEG4000-g-SiO_2. The scale bar in (a-c) is 500 nm. (d-h) are the particle enlarged TEM images of SiO_2 nanoparticles: (d) SiO_2; (e-f) MPEG750-g-SiO_2; (g) MPEG2000-g-SiO_2 and (h) MPEG4000-g-SiO_2. The scale bar in (d,e,g,h) is 100 nm and the scale bar in (f) is 50 nm. (i) SAXS scattering profiles of MPEG-g-SiO_2 at 90 °C. The curves are arbitrarily shifted for clarity.*

Non-Isothermal Crystallization Behavior of Grafted MPEG

Figures 2a through 2c show the non-isothermal crystallization behavior of MPEG750-*g*-SiO_2, MPEG2000-*g*-SiO_2 and MPEG4000-*g*-SiO_2, as a function of σ

(the ranges of grafting density are shown in Fig. S2 and Table S1). Figures 2 d-f show the influence of grafting density on T_c, X_c and T_m. The DSC melting scans (shown in Figure S3) and crystallization behavior of MPEG*x*-*g*-SiO_2 with three different molecular weights exhibit similar trends. It is obvious that the variations of X_c, T_c and T_m are dependent on the grafting density.

Figure 2a through 2c show how the peak crystallization temperature, T_c, of grafted chains decreases gradually as grafting density decreases. It must be remembered that the lower the grafting density, the higher the amount of silica in the nanocomposites (Figure 3). It is also worth noting that the range of silica contents employed in this work are always above 68 % and can be as high as 85 % (the volume fraction of SiO_2 ranges from 53.4 vol % to 74.5 vol %) depending on the grafting degree (Figure 3). Therefore, it is not surprising that even at the lowest silica contents (i.e., maximum grafting degrees) the crystallization temperature is lower than the corresponding value for the parent homopolymer.

The crystallization of grafted PEO is seriously hindered by the confinement effects introduced by decreasing grafting density (increasing contents of SiO_2). The enthalpy of crystallization also decreases as grafting density decreases and for the lowest molecular weight of the grafted MPEG chains, the samples cannot crystallize during cooling from the melt (at 10 ºC/min) when the grafting density decreases to $\sigma \leq 1.78$ (and the silica content increases). At the lowest grafting density, the SiO_2 content is as high as 74.5 vol % (85 wt %), which is high enough to form packed spheres. In that case, the grafted chains should be tightly bound on the SiO_2 surface

(as a result of the very large surface area available), resulting in a strong suppression of crystallization.

A general comparison of the crystallinity degree, T_c and T_m values as a function of grafting density, for all three molecular weight samples, is presented in Figures 2d-2f. The effects of gradually decreasing grafting density (and at the same time increasing silica content) are equivalent to a gradual increase in confinement.

Both T_c and T_m are greatly depressed with decreases in grafting density, but the shift in T_c values to lower temperatures is generally twice as large as the decrease in T_m values. The melting point values are only affected by the lamellar thickness of the crystals developed during cooling (and reorganized during heating, if any reorganization takes place). However, T_c values depend on nucleation density (a cooling rate dependent value) and on possible changes in nucleation mechanisms due to confinement. Additionally, the degree of crystallinity decreases dramatically, as the grafting density decreases.

Similar trends of decreasing thermal transitions and crystallinity have been reported for nanocomposites with carbon nanotubes, when the amount of nanofillers increase well beyond their percolation threshold inducing confinement effects[48].

Figures 2 and 3 allow us to establish the influence of molecular weight on the crystallization and melting behavior of grafted MPEG chains onto silica. If a constant grafting density of 0.7 is taken in Figure 3, as an example, it can be observed that the content of silica increases when the molecular weight of the grafted chains reduces from 4000 to 750 g/mol. Then it is easy to understand why, the crystallization ability

of the sample MPEG750-g-SiO_2 is the one more affected, followed by the MPEG2000-g-SiO_2 and finally by the MPEG4000-g-SiO_2 sample. The lower the molecular weight of the grafted chains, the highest the impact of reducing grafting density on chain crystallizability.

The interfacial interaction (that increases with decreases in grafting density) is the dominant factor that affects the mobility of grafted chains and influences their crystallization behavior. The suppressed crystallization in MPEG750-*g*-SiO_2 at low grafting density is caused by confinement effects introduced by the large amount of SiO_2.[21, 37] The grafted MPEG chains with lower M_n are more confined and more difficult to stretch out on SiO_2-NH_2 surfaces than when they are in the bulk. At lower grafting density, the high SiO_2 contents induce more MPEG chains to bind to the surfaces of neighboring particles with much stronger interfacial interaction (covalent bonding and hydrogen bonding effects). These attractive interactions between SiO_2 and grafted MPEG chains cause a decrease in chain mobility and an increase in the glass transition temperature (T_g), that result in a strong suppression of crystallization.

Our experimental results have similar trends as those reported previously by some of us[37] in a related but different system, where PEO chains were physically adsorbed on SiO_2. It was found that higher SiO_2 content also brings stronger confinement effects with a turning point at around 70 wt % SiO_2. Beyond 70 wt % SiO_2, the nanoparticles could form a closed packed sphere assembly constituted by the directly connected SiO_2 network structure.

The crystallization behavior of MPEG*x*-*g*-SiO_2 has a large dependence on the

degree of confinement as will be discussed in detail below.

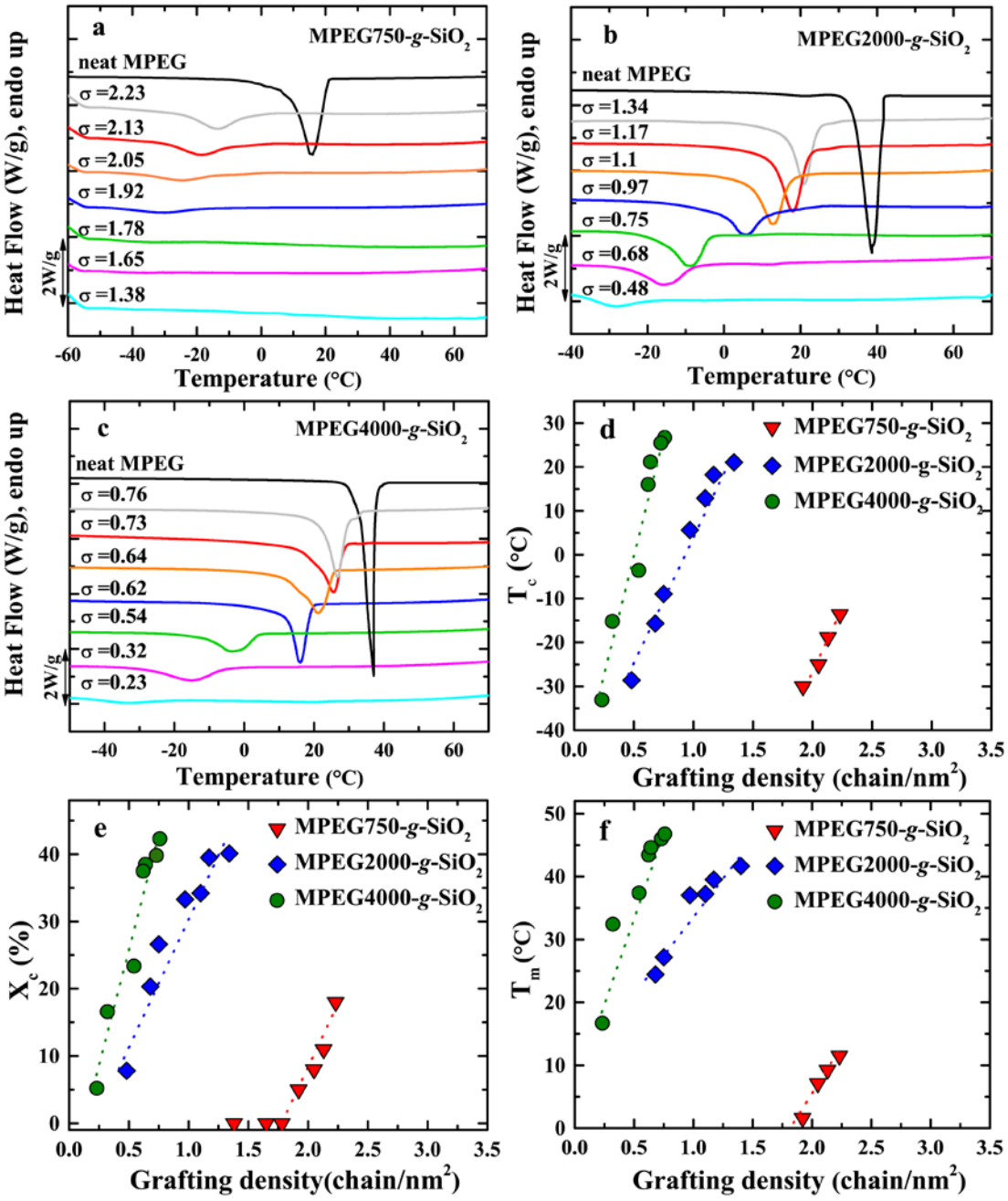

FIGURE 2. *(a-c) DSC cooling scans for the indicated MPEGx-g-SiO₂. (d-f) Influence of grafting density on T_c, X_c and T_m of MPEGx-g-SiO₂.*

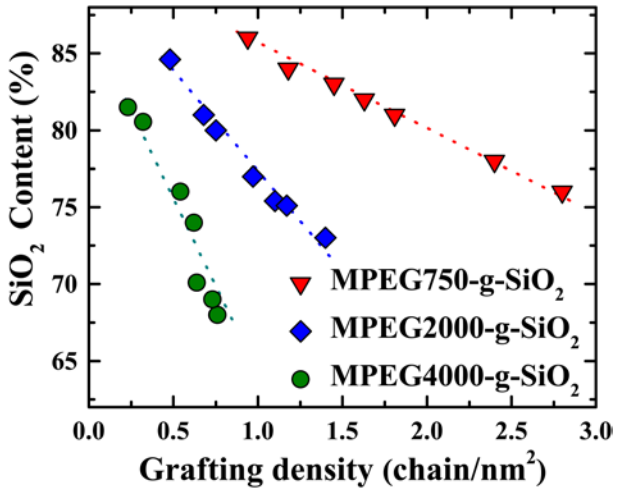

FIGURE 3. *Relationship between silica content and grafting density*

The crystal structure of MPEG is not affected by the silica content. WAXS studies were performed and are reported in Fig. S4 of the Supporting Information proving that the monoclinic unit cell of neat MPEG is preserved in the nanocomposites.

Self-Nucleation Behavior of the grafted MPEG chains onto silica

Fillon et al. proposed a DSC thermal protocol to study self-nucleation (SN) in isotactic polypropylene.[42] The method has been applied by Müller et al. to study confined crystallization in copolymers and nanocomposites, amongst other polymeric systems.[43, 49] The self-nucleation technique was employed to explore if confinement of grafted chains could affect their self-nucleation behavior.

Due to the large confinement effects detected in MPEG750-*g*-SiO_2, as shown in Figure 2a, no heat flow signal could be detected at lower grafting density. Therefore, we mainly focus on the self-nucleation behavior of MPEG2000-*g*-SiO_2 and MPEG4000-*g*-SiO_2.

Figures 4a and 4b show the DSC cooling and subsequent melting scans of neat

MPEG2000 during self-nucleation at different self-nucleation temperatures (T_s). Neat MPEG2000 exhibits the standard SN behavior and displays the three SN Domains.[43]

Figures 4c and 4e illustrate the self-nucleation behavior of MPEG2000-*g*-SiO_2 with σ = 1.34 and 1.17, respectively. When σ = 1.34, the sample is in *Domain I* (complete melting) when the T_s temperature is equal or higher than 55 °C, as the crystallization occurs at the same T_c value as in neat MPEG2000. *Domain II* (self-nucleation)[43] occurs in a T_s range between 52 and 47 °C, as the peak T_c values increase slightly (Figure 4c), while the subsequent melting traces reveal no traces of annealing (Figure 4d). For $T_s \leq$ 45 °C, a sharp endothermic peak is detected in the subsequent melting endotherm, which indicates that the sample is in *Domain III* (self-nucleation and annealing) (Figure 4d), as the second or high temperature melting peak correspond to the fusion of the crystals annealed at the corresponding T_s value (i.e., 45 ºC in Figures 4c and 4d).

The self-nucleation capacity of grafted MPEG chains disappears when the grafting density decreases below a certain degree. Figure 4e shows the absence of *Domain II* when the grafting density decreased to σ = 1.17. The same change in the self-nucleation behavior was also obtained for MPEG4000-*g*-SiO_2 (as shown in Fig. S5, Supporting Information).

The self-nucleation behavior of MPEG2000-g-SiO_2 and MPEG4000-g-SiO_2 (Fig. S5, Supporting Information) with different grafting density are schematically represented in Table 1 (the green range indicates the disappearance of *Domain II*) and the typical descriptions of three domains are summarized in Figure S6. The grafted

MPEG with higher grafting density can be self-nucleated, in a rather similar way to neat MPEG. The grafted MPEG with lower grafting density exhibits the absence of *Domain II* (green region in Table 1), indicating a highly confined crystallization.

The absence of *Domain II* has been previously reported for strongly segregated block copolymer systems, in cases where the microphase segregated phases are highly confined (like in spherical or cylindrical microdomains).[16, 50-52] The absence of *Domain II* has also been detected in nanocomposites with high contents of carbon nanotubes.[43, 53] Therefore, the SN results obtained here support that the decrease of grafting density strongly confines the crystallization of the grafted MPEG chains. When the confinement effects are strengthened with large decreases of grafting density, they lead to the eventual disappearance of self-nucleation or *Domain II*.

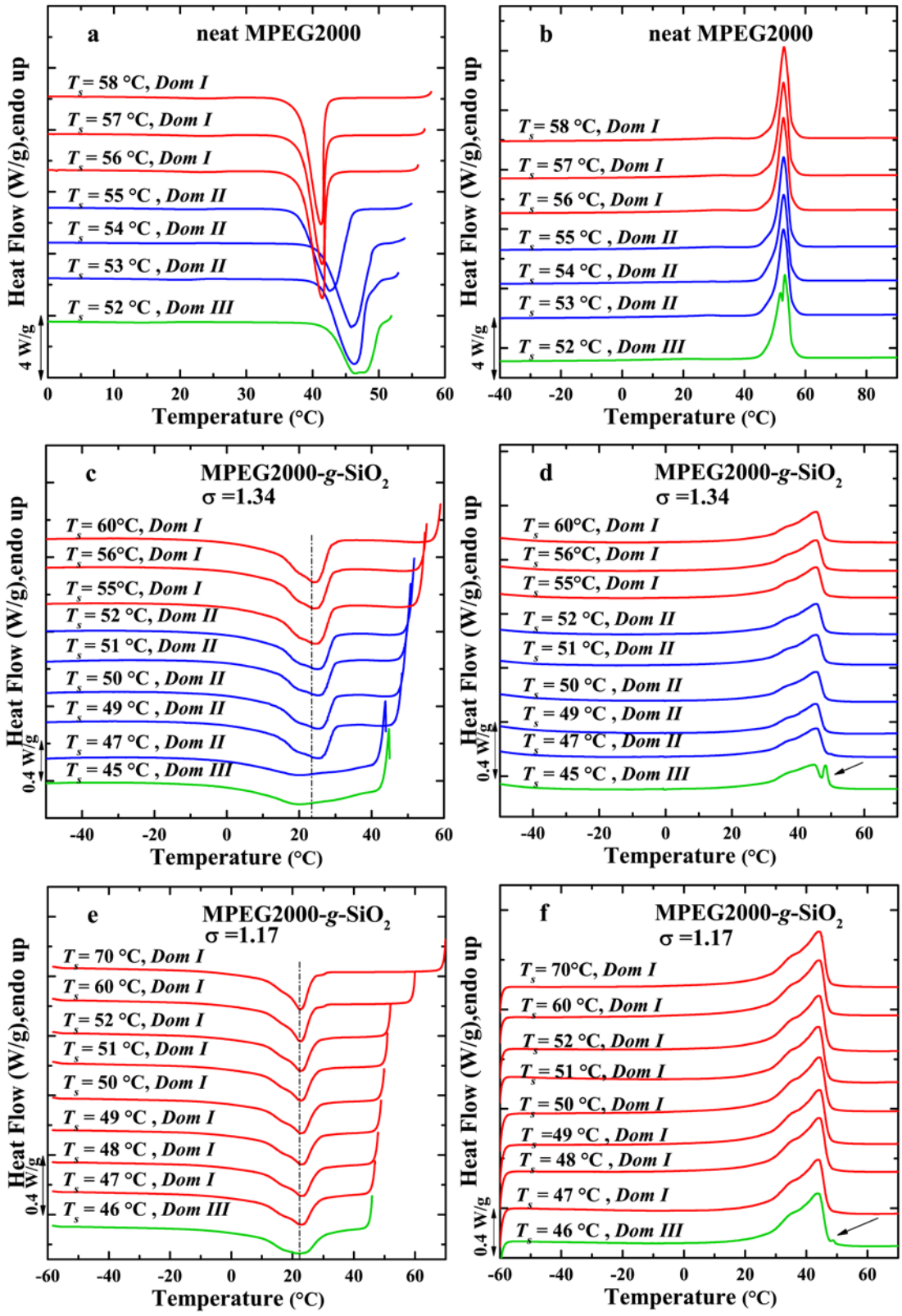

FIGURE 4. *(a, c, e) DSC cooling scans for neat MPEG2000, σ = 1.34 and σ = 1.17 of MPEG2000-g-SiO_2 after self-nucleation at the indicated T_s; (b, d, f) subsequent heating scans for neat MPEG2000 and for MPEG2000-g-SiO_2 with σ = 1.34 and σ = 1.17.*

TABLE 1 *Dependence of Self-Nucleation Behavior on Grafting Density of MPEGx-g-SiO₂*

	Grafting density(chains/nm^2)				
Samples	**< 0.62**	**0.62**	**1.17**	**1.34**	**0 (neat MPEG)**
MPEG2000-g-SiO₂	**two domains (I III)**	**two domains (I III)**	**two domains (I III)**	**three domains (I II III)**	**three domains (I II III)**
MPEG4000-g-SiO₂	**two domains (I III)**	**three domains (I II III)**			**three domains (I II III)**

Isothermal Crystallization Behavior of Grafted MPEG chains onto silica

As mentioned in the experimental section, we employ the isothermal step crystallization (ISC) experiments[39] for grafted polymers. The unique advantage of isothermal step crystallization makes possible to get information of different crystallization processes at a given T_c and to extend the temperature range when isothermal crystallization is performed.[40]

Figure 5 illustrates the overall isothermal crystallization behavior of neat MPEG2000 and MPEG2000-*g*-SiO_2 with σ = 1.34. The solid lines are the Avrami fitting curves, from which we can obtain the Avrami index (n). Müller et al.[40] proposed that the Avrami index can be considered the sum of two parts:

$$\boldsymbol{n = n_n + n_{gd}} \quad (5)$$

where $\boldsymbol{n_n}$ is the fraction of the index related to nucleation ($\boldsymbol{n_n}$ has limiting values of 0 for instantaneous nucleation and 1 for sporadic nucleation) and $\boldsymbol{n_{gd}}$ corresponds to growth dimensionality (where the typical variation range is 1-3, although most bulk polymers form axialites (2D) or spherulites (3D)). In most cases, for bulk polymers

forming spherulites, because the nucleation may be between completely instantaneous ($\boldsymbol{n_n} = 0$) or sporadic ($\boldsymbol{n_n} = 1$), Avrami indices between 3 and 4 are usually obtained. For neat MPEG2000 (Figure 5a) the Avrami index is between 3 and 4. On the other hand, for grafted MPEG chains (Figure 5b), the value is reduced to around 1.5 which indicates instantaneous axialites are being formed of grafted chains as compared to the neat MPEG.

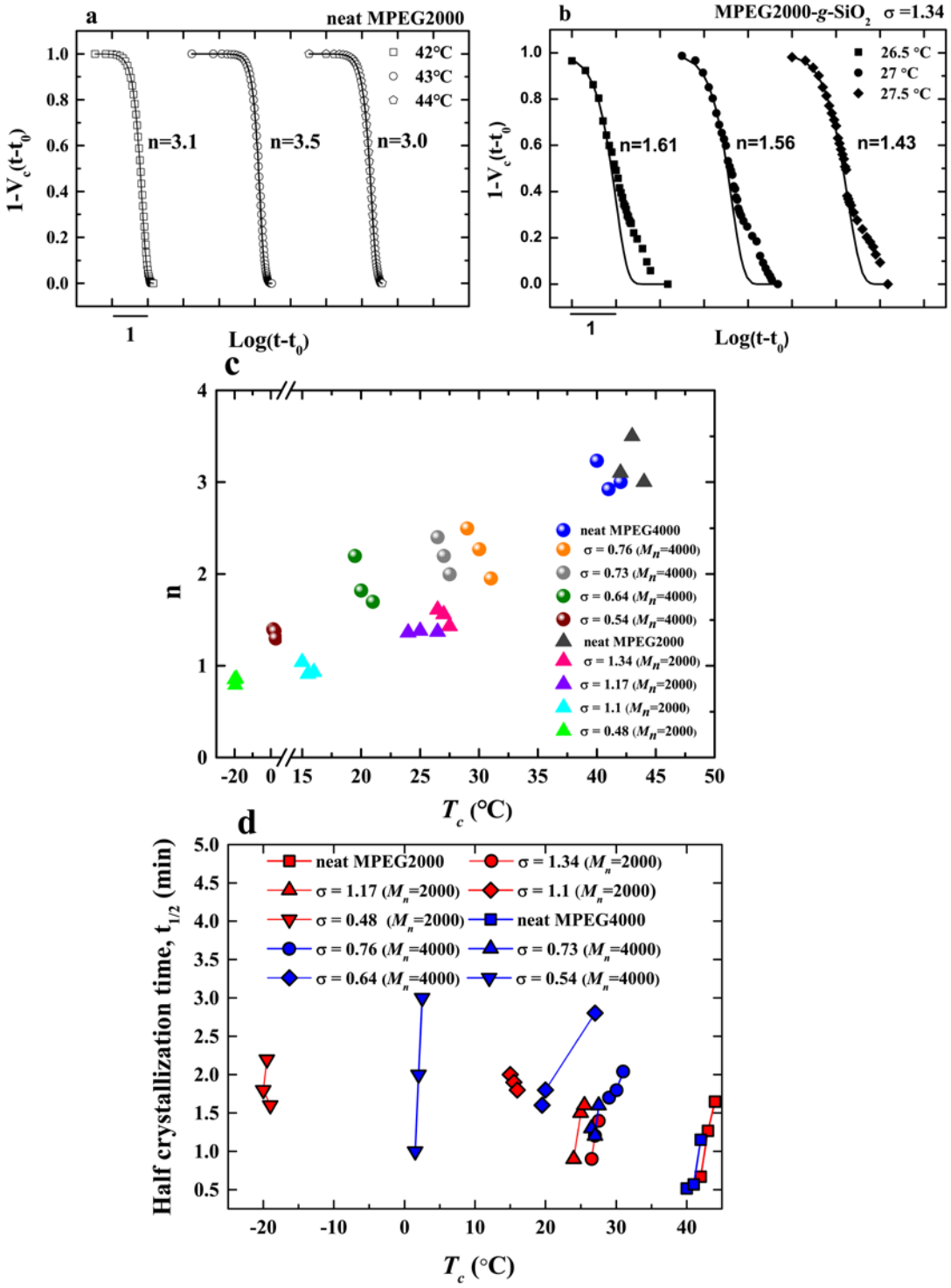

FIGURE 5. *(a-b) Avrami fitting curves (solid lines) for neat MPEG2000 and MPEG2000-g-SiO₂ of σ=1.34 at the specified crystallization temperatures. (c) relationship between Avrami index of MPEGx-g-SiO₂ composites and isothermal crystallization temperature. (d) crystallization half-time, $t_{1/2}$, as a function of isothermal crystallization temperature for neat MPEG and for*

MPEGx-g-SiO_2.

The Avrami index values of MPEG*x*-*g*-SiO_2 with different grafting density are summarized in Figure 5c. (Avrami fits for neat MPEG4000 and MPEG4000-*g*-SiO_2 are shown in Fig. S7, Supporting Information). The Avrami indices of the MPEG*x*-*g*-SiO_2 exhibit a decreasing trend with the decrease of grafting density due to the increasing confinement degree on SiO_2-NH_2. The correlation between Avrami index and confinement is remarkable and this is the first time it has been obtained in PGNPs nanocomposites. Similar trends have been reported previously for different confined materials, such as block copolymer nanophases or nanocomposites containing carbon nanotubes.[16-17, 48]

It cannot be ignored that as confinement increases, the nanocomposites need higher degrees of supercooling in order to crystallize. The confinement degree increases with the decrease of grafting density and confined chains need larger supercoolings to form crystals.[40]

A strong confinement effect usually induces a nucleation control over the overall crystallization kinetics, or in other words $\boldsymbol{n_n} >> \boldsymbol{n_{gd}}$. The Avrami index can then be in the nucleation-controlled regime between 0 (for sporadic nucleation) and 1 (for a first order crystallization kinetics, determined by sporadic nucleation). First order crystallization kinetics (*n* values of approximately 1) have been obtained for the confined crystallization of block copolymers, droplets, polymer blends, infiltrated polymers within alumina nanoporous templates and nanocomposites.[16-17, 48, 54-56]

When the grafting density decreases to a certain degree, such as σ = 0.48 of

MPEG2000-*g*-SiO_2, the Avrami index was less than 1, implying that nucleation is not completely sporadic but is in between sporadic and instantaneous. Similar low values of *n* have aslo been reported in the study of confined crystallization of polymers in droplets, nanocomposites with carbon nanotubes, infiltrated polymers in nanoporous alumina templates and block copolymers.[57-59]

Another important observation that can be made from Figure 5 is that very low T_c values had to be employed in order to crystallize the nanocomposites with higher degrees of confinement (even -20 ºC). This is consistent with very low peak crystallization temperatures when highly confined materials are cooled from the melt in Figure 2. The crystallization peak (Figure 2) shifted to $T_c \approx$ -30 ºC which is close to the T_g of MPEG at low grafting density. If we consider this evidence together with the absence of *Domain II* and the Avrami index values of 1 or lower, we arrive at the conclusion that the MPEG chains for the highly confined cases described above are being nucleated homogeneously. In fact, PEO is one of the few polymers were homogenous nucleation has been extensively reported for confined isolated phases.[16-17, 51-52, 55, 60]

The plots of crystallization half-time ($t_{1/2}$), which is inversely related to the crystallization rate, for neat MPEG and MPEG*x*-*g*-SiO_2 are shown in Figure 5d. The overall crystallization rate is related to the grafting density both in MPEG2000-*g*-SiO_2 and MPEG4000-*g*-SiO_2. The data presents large scattering due to the difficulty in the determination of the overall crystallization kinetics, as the degree of crystallinity is reduced with confinement. Only a few crystallization temperatures were used to

determine the crystallization kinetics employing the ISC method.

Two general observations can be made from Figure 5d: (a) the degree of supercooling needed for crystallization increases with confinement and (b) a general trend of reducing the crystallization rate (increasing the half-crystallization time) is apparent in Figure 5d as confinement increases, especially if one tries to compare data at identical T_c values by extrapolating the observed trends of the few data points represented. In summary, the overall crystallization rate of MPEG*x*-*g*-SiO_2 decreases with the decrease of grafting density, which derives from the enhanced confinement effects at low grafting density. The results are consistent with the non-isothermal crystallization experiments presented above in Figure 2.

Interfacial Interaction of Grafted MPEG Chains with SiO_2

To further characterize the confinement degree of grafted chains on SiO_2-NH_2, derivative TGA (dTGA)[14, 61-62] was employed to study the interfacial interaction between grafted MPEG and SiO_2-NH_2. Figure 6 presents the dTGA curves of the MPEG*x*-*g*-SiO_2 with different molecular weights. All three different molecular weights samples of MPEG*x*-*g*-SiO_2 exhibit higher thermal decomposition temperature than neat MPEG. The MPEG2000-*g*-SiO_2 nanocomposites behavior will be explained below in detail as an example.

The characteristic thermal decomposition temperature of neat MPEG2000 is 392 ^oC, taken as the maximum of the dTGA curve, whereas the MPEG2000-*g*-SiO_2 always exhibits a higher decomposition temperature than neat MPEG2000. With an increase

of grafting density, the decomposition temperature decreases but it is still higher than neat MPEG even at the highest grafting density (i.e., σ = 1.34), a result of the strong interfacial interaction between grafted MPEG chains and SiO_2-NH_2.

On the one hand, the MPEG chains are immobilized on the surface of SiO_2-NH_2 by chemical bonding. This leads to the enhancement of interfacial interaction between the grafted chains and SiO_2-NH_2 and to the improvement of the thermal stability of grafted MPEG. On the other hand, there are a number of unhydrolyzed ethoxy groups and hydroxyl groups formed by hydrolysis on the surface of SiO_2-NH_2, which can easily form hydrogen bonds with the ether oxygen bonds present in the repeating units of MPEG.[62]

At lower grafting density, the grafted chains are tightly bound to the surface of SiO_2-NH_2, and as discussed above, the interfacial interaction with MPEG chains is stronger and the crystallization ability of these chains becomes strongly impaired. On the other hand, the covalent bonding effects between MEPG and SiO_2-NH_2 become weakened and the decomposition temperature of the nanocomposites decreases with the increase of the grafting density. Therefore, the grafted chains at higher grafting density have a smaller degree of confinement and their crystallization ability is enhanced (Figure 2), while their decomposition temperature is lower.

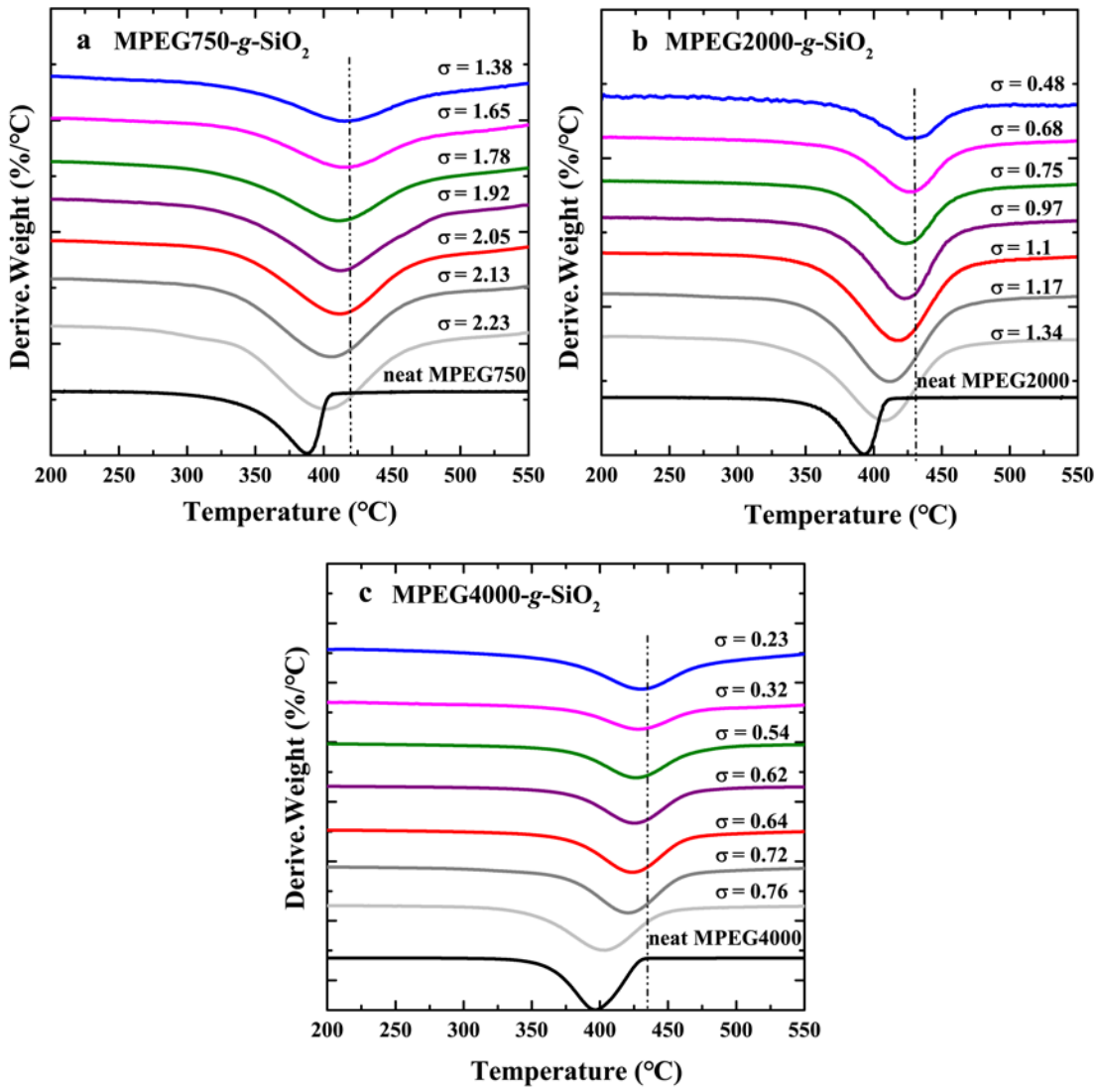

FIGURE 6. *(a-c) dTGA curves of MPEG750-g-SiO_2, MPEG2000-g-SiO_2 and MPEG4000-g-SiO_2 with different grafting density.*

Characterization of Confinement Degree on SiO_2-NH_2

The crystallization behavior of grafted chains has a large dependence on the conformation of the chains in a confined environment. In order to evaluate such conformational effects, the surface coverage of grafted MPEG on SiO_2-NH_2 can be used as an approximate measurement of some conformational parameters related to the size of the chains.

Wunder et al.[14] studied the surface coverage of grafted PEO layer on SiO_2, which is determined by two parameters: (a) the average radius of gyration (R_g) of the chains in theta (Θ) conditions and (b) the surface radius (R_s) occupied by one chain on the surface of SiO_2-NH_2. The value of R_s/R_g can be used as a measurement of the confinement degree of the grafted chains on SiO_2-NH_2.

The radius of gyration R_g is normally determined in solution, and it provides a measure of the size of the polymeric coil,[14] It can be obtained according to the following formula:

$$R_g = (Nb_{PEG}^2/6)^{1/2} \quad (6)$$

where b_{PEG} is the Kuhn length of MPEG and its value is 11 Å, N represents the number of freely-jointed effective bonds of length b_{PEG}. The R_g of neat MPEG with molecular weight 750, 2000 and 4000 g mol^{-1} calculated by the above formula are 10.5 Å, 17.1 Å and 24.3 Å, respectively. Because the dimensions of the grafted chains are small as compared to the size of SiO_2-NH_2 nanoparticles (i.e., 500 Å), we have assumed that the surface area is occupied by a single MPEG chain on SiO_2-NH_2 .This is similar to the case of two-dimensional films whose surface area would be given by $A_{surface} = \pi R_s$.[2 14] The grafting density (chains/nm^2) is used to normalize the $A_{surface}$, through which R_s can be obtained. The ratio of R_s/R_g represents the confinement degree and is related to the interfacial properties of grafted MPEG.

As shown in Table 2**,** the decreasing trend of R_s/R_g with the increase of grafting density indicates that the chains become less spread on the particle surface (i.e., more compact with respect to one another) with their non-grafted chain ends oriented away

from the surface of the SiO_2-NH_2 nanoparticles. Therefore, the interfacial interaction between grafted MPEG and SiO_2-NH_2 is substantially reduced while the mobility and crystallization ability are both enhanced as grafting degree increases.

The stretching properties of grafted chains can be described by the dependence of the distance between grafting sites D on $2R_g$,[63] where D is calculated using:[64]

$$D = (4/\pi\sigma)^{1/2} \quad (7)$$

If $D > 2R_g$, the individual chains cannot interact with adjacent chains and form mushroom conformations. When the grafted chains begin to overlap ($D \leqslant 2R_g$), they behave as brushes stretching away from the particle surface.[63, 65] In the case of MPEG*x*-*g*-SiO_2, the value of $D/2R_g$ is equivalent to the ratio of R_s/R_g ($R_s = (1/\pi\sigma)^{1/2}$). The interchain spacings for grafted chains are all lower than $2R_g$ (i.e., $R_s/R_g < 1$, as shown in Table 2). The value of R_s/R_g decreases from 0.48 at lower grafting density of low molecular weight chains (MPEG2000-*g*-SiO_2, σ = 0.48 chains/nm^2) to 0.26 at higher grafting density of high molecular weight chains (MPEG4000-*g*-SiO_2, σ = 0.76 chains/nm^2), which indicates that the grafting chains are in the "brush region".[66] The dimensions of the grafted chains in nanocomposites with the maximum grafting degrees (i.e., the lowest SiO_2 content in Figure 3) tend to be more brush-like with chain ends oriented away from the SiO_2-NH_2.[21]

TABLE 2 *The Relationship between R_s/R_g and Grafting Density*

	Weight Loss (%)	*Grafting Density (chains /nm^2)*	*R_s (Å)*	*R_g (Å)*	*R_s/R_g*
750	8.6	1.38	4.80	10.5	0.46
	9.1	1.65	4.39		0.42
	10.8	1.78	4.23		0.40
	11.6	1.92	4.07		0.39

	12.0	2.05	3.94		0.38
	12.7	2.13	3.87		0.37
	13.2	2.23	3.78		0.36
	8	0.48	8.14		0.48
	11	0.68	6.84		0.40
	12	0.75	6.52		0.38
2000	15	0.97	5.73	17.1	0.34
	17	1.10	5.38		0.31
	17.5	1.17	5.22		0.30
	19.6	1.34	4.88		0.29
	7.5	0.23	11.7		0.48
	10	0.32	9.98		0.41
	16	0.54	7.68		0.32
4000	18	0.62	7.11	24.3	0.29
	19	0.64	7.05		0.29
	21	0.73	6.61		0.27
	23	0.76	6.47		0.26

A schematic model based on the different grafting densities of MPEG*x*-*g*-SiO_2 samples combined with the DSC, TGA and WAXS results obtained here is proposed in Figure 7, in order to describe the relationship between crystallization behavior and grafting density.

At lower grafting densities, one end of the grafted MPEG chain is fixed on the SiO_2-NH_2 nanoparticle surface by a chemical bond, while the ether oxygen in the ether group belonging to the other chain free end forms a hydrogen bond with a silanol group of the SiO_2-NH_2 nanoparticle. The grafted MPEG chains are tightly bound to the surface of nanoparticles, resulting in large topological restrictions that significantly affect the crystallization ability of these grafted chains. Moreover, the lower crystallization temperature and crystallinity obtained from the DSC analysis (Figure 2) are in good agreement with the poor ability to crystallize of the grafted MPEG with low grafting densities. In addition, the low Avrami index determined by

isothermal crystallization measurement further demonstrated the confined crystallization behavior of the grafted chains at low grafting densities.

When the grafting density is increased to a moderate degree, the space occupied by a single chain on the surface of SiO_2-NH_2 particles is reduced. Some part of grafted chains with ether oxygen bonds will be tightly bound to the hydroxyl groups (silanol, ≡Si−OH), but others will tend to be away from the SiO_2-NH_2 nanoparticle surface and will easily crystallize with adjacent chains.

At the higher grafting densities, the dimensions occupied by the grafted chains on the surface of the nanoparticles are further reduced. The majority of the chains will be away from SiO_2-NH_2 surfaces, and in this case, the grafted chains have the lowest topological confinement and hence the strongest crystallization ability.[14] Therefore, the crystallization temperature, crystallinity and the Avrami index of grafted MPEG show an increasing trend with grafting density increases.

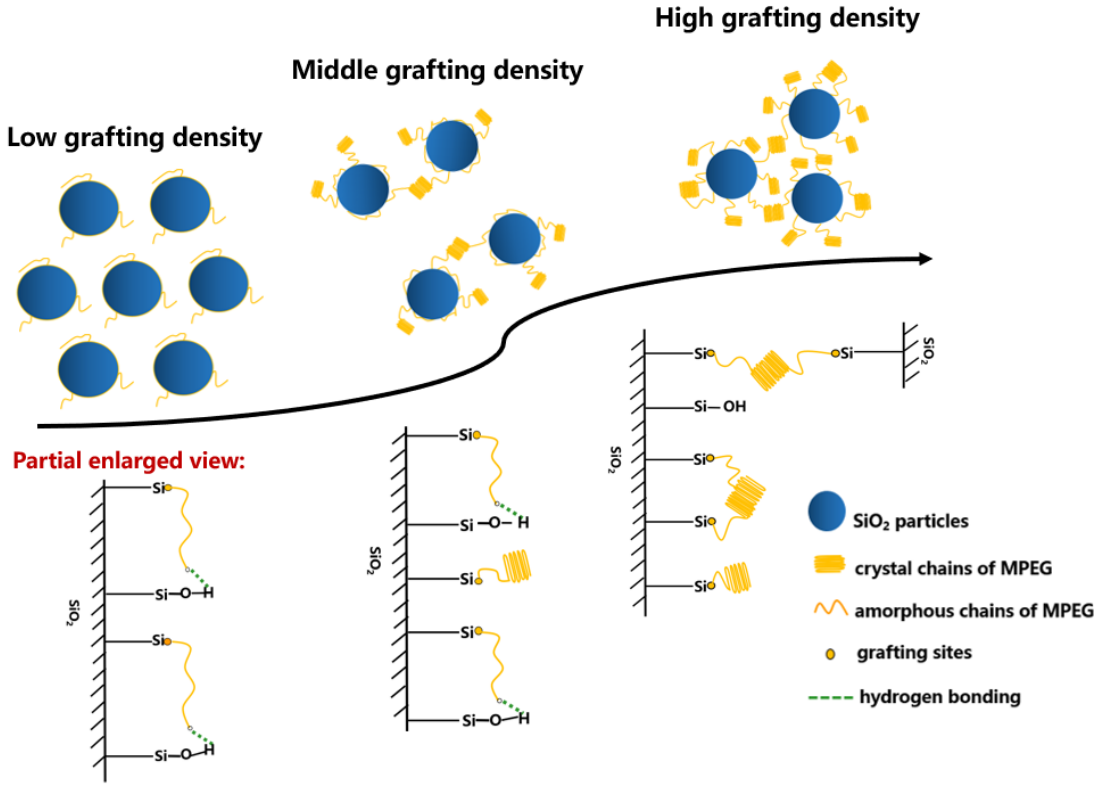

FIGURE 7. *Schematic illustration of MPEG chains on SiO_2-NH_2*

CONCLUSIONS

We have systematically investigated the confined crystallization of grafted MPEG chains onto silica nanoparticles by varying the grafting density and polymer molecular weight using DSC, TGA, and WAXS techniques.

The confinement effects which affect the mobility and crystallization behavior of grafted MPEG chains are stronger for lower molecular weight of MPEG chains. As the grafting density decreases, the crystallinity of grafted MPEG chains decreases dramatically. In the case of low grafting density, the confinement effects are strengthened and lead to the eventual disappearance of *Domain II*.

The Avrami indices (n) of the MPEGx-g-SiO_2 exhibit a decreasing trend with the decrease of grafting density due to the increasing confinement degree of SiO_2-NH_2

content. When the grafting density decreases below a certain degree (and the silica content increases), the Avrami index values of the MPEG*x*-*g*-SiO_2 are less than 1. During non-isothermal crystallization from the melt of these very low grafting degree samples, the crystallization temperature peak shifts to $T_c \approx$ -30 ºC (i.e., close to the T_g of MPEG) indicating that MPEG chains for these highly confined cases are being nucleated homogeneously.

The enhanced interfacial interaction at low grafting density strongly impairs the crystallization ability of MPEG chains. Theoretical calculations demonstrated that the grafted MPEG chains are tightly bound to the surface of SiO_2 at low grafting density, resulting in large topological restrictions that significantly affect the crystallization ability of these grafted chains.

ACKNOWLEDGMENTS

This project was supported by the National Natural Science Foundation of China (21574141) and the Ministry of Science and Technology of China (2017YFE0117800). The authors gratefully acknowledge the funding of project BIODEST, Research and Innovation Staff Exchange (RISE) H2020-MSCA-RISE-2017-778092. The authors thank beamline BL16B1 (Shanghai Synchrotron Radiation Facility) for providing the beam time and helps during experiments.

REFERENCES AND NOTES

1. Honma, I.; Nomura, S.; Nakajima, H., Protonic conducting organic/inorganic nanocomposites for polymer electrolyte membrane. *J Membrane Sci* **2001,** *185*, 83−94.
2. Ahmadi-Moghadam, B.; Sharafimasooleh, M.; Shadlou, S.; Taheri, F., Effect of functionalization of graphene nanoplatelets on the mechanical response of graphene/epoxy composites. *Mater Design* **2015,** *66*, 142−149.
3. Xu, B.; Song, Y. H.; Zheng, Q., Molecular relaxation and rheological behaviors of fumed silica/low-molecular weight polyethylene glycol suspensions. *Acta Polym Sin* **2017,** *11*, 1832−1840.
4. Chen, J.; Bi, H.; Sun, S. R.; Tang, Y. F.; Zhao, W.; Lin, T. Q.; Wan, D. Y.; Huang, F. Q.; Zhou, X. D.; Xie, X. M.; Jiang, M. H., Highly conductive and flexible paper of 1D silver-nanowire-doped graphene. *ACS Appl Mater Inter* **2013,** *5*, 1408−1413.
5. Qi, J. J.; Lv, W. P.; Zhang, G. L.; Zhang, F. B.; Fan, X. B., Poly(N-isopropylacrylamide) on two-dimensional graphene oxide surfaces. *Polym Chem* **2012,** *3*, 621−624.
6. Shenhar, R.; Norsten, T. B.; Rotello, V. M., Polymer-mediated nanoparticle assembly: Structural control and applications. *Adv Mater* **2005,** *17*, 657−669.
7. Li, Q.; Dong, L. J.; Fang, J. F.; Xiong, C. X., Property-structure relationship of nanoscale ionic materials based on multiwalled carbon nanotubes. *ACS Nano* **2010,** *4*, 5797−5806.
8. Hasegawa, R.; Aoki, Y.; Doi, M., Optimum graft density for dispersing particles in polymer melts. *Macromolecules* **1996,** *29*, 6656−6662.
9. Jia, X. L.; Listak, J.; Witherspoon, V.; Kalu, E. E.; Yang, X. P.; Bockstaller, M. R., Effect of matrix molecular weight on the coarsening mechanism of polymer-grafted gold nanocrystals. *Langmuir* **2010,** *26*, 12190−12197.
10. Srivastava, S.; Agarwal, P.; Archer, L. A., Tethered nanoparticle-polymer composites: phase stability and curvature. *Langmuir* **2012,** *28*, 6276−6281.
11. Francis, R.; Joy, N.; Aparna, E. P.; Vijayan, R., Polymer grafted inorganic nanoparticles, preparation, properties, and applications: A review. *Polym Rev* **2014,** *54*, 268−347.
12. Savin, D. A.; Pyun, J.; Patterson, G. D.; Kowalewski, T.; Matyjaszewski, K., Synthesis and characterization of silica-graft-polystyrene hybrid nanoparticles: Effect of constraint on the glass-transition temperature of spherical polymer brushes. *J Polym Sci Pt B-Polym Phys* **2002,** *40*, 2667−2676.
13. Maillard, D.; Kumar, S. K.; Rungta, A.; Benicewicz, B. C.; Prudhome, R. E., Polymer-grafted-nanopartice surfactants. *Nano Letters* **2011,** *11*, 4569−4573.
14. Maitra, P.; Ding, J.; Huang, H.; Wunder, S. L., Poly(ethylene oxide) silananted nanosize fumed silica: DSC and TGA characterization of the surface. *Langmuir* **2003,** *19*, 8994−9004.
15. Nakagawa, S.; Kadena, K.; Ishizone, T.; Nojima, S.; Shimizu, T.; Yamaguchi, K.; Nakahama, S., Crystallization behavior and crystal orientation of

poly(ε-caprolactone) homopolymers confined in nanocylinders: effects of nanocylinder dimension. *Macromolecules* **2012,** *45*, 1892−1900.
16. Müller, A. J.; Balsamo, V.; Arnal, M. L., Nucleation and crystallization in diblock and triblock copolymers. *Adv Polym Sci* **2005,** *190*, 1−63.
17. Michell, R. M.; Müller, A. J., Confined crystallization of polymeric materials. *Prog Polym Sci* **2016,** *54−55*, 183−213.
18. Lin, M. C.; Nandan, B.; Chen, H. L., Mediating polymer crystal orientation using nanotemplates from block copolymer microdomains and anodic aluminium oxide nanochannels. *Soft Matter* **2012,** *8*, 7306−7322.
19. Rottele, A.; Thurn-Albrecht, T.; Sommer, J. U.; Reiter, G., Thermodynamics of formation, reorganization, and melting of confined nanometer-sized polymer crystals. *Macromolecules* **2003,** *36*, 1257−1260.
20. Liu, X. B.; Zhao, Y. F.; Fan, X. H.; Chen, E. Q., Crystal orientation and melting behavior of poly (ε-Caprolactone) under one-dimensionally "hard" confined microenvironment. *Chin J Polym Sci* **2013,** *31*, 946−958.
21. Kim, S. A.; Archer, L. A., Hierarchical structure in semicrystalline polymers tethered to nanospheres. *Macromolecules* **2014,** *47*, 687−694.
22. Zhou, B.; Tong, Z. Z.; Huang, J.; Xu, J. T.; Fan, Z. Q., Isothermal crystallization kinetics of multi-walled carbon nanotubes-graft-poly(epsilon-caprolactone) with high grafting degrees. *CrystEngComm* **2013,** *15*, 7824−7832.
23. Zhou, B.; He, W. N.; Jiang, X. Y.; Tong, Z. Z.; Xu, J. T.; Fan, Z. Q., Effect of molecular weight on isothermal crystallization kinetics of multi-walled carbon nanotubes-graft-poly(epsilon-caprolactone). *Compos Sci Technol* **2014,** *93*, 23−29.
24. Jana, R. N.; Cho, J. W., Thermal stability, crystallization behavior, and phase morphology of poly(epsilon-caprolactone)diol-grafted-multiwalled carbon nanotubes. *J Appl Polym Sci* **2008,** *110*, 1550−1558.
25. Dukes, D.; Li, Y.; Lewis, S.; Benicewicz, B.; Schadler, L.; Kumar, S. K., Conformational transitions of spherical polymer brushes: synthesis, characterization, and theory. *Macromolecules* **2010,** *43*, 1564−1570.
26. Hommel, H.; Legrand, A. P.; Tougne, P.; Balard, H.; Papirer, E., Influence of the grafting ratio on the conformations of poly(ethylene oxide) chains grafted on silica. *Macromolecules* **1984,** *17*, 1578−1581.
27. Yu-Su, S. Y.; Sheiko, S. S.; Lee, H. I.; Jakubowski, W.; Nese, A.; Matyjaszewski, K.; Anokhin, D.; Ivanov, D. A., Crystallization of molecular brushes with block copolymer side chains. *Macromolecules* **2009,** *42*, 9008−9017.
28. Zhao, Z. F.; Liu, P. Y.; Zhang, C. Q.; Liu, W.; Wang, Y. H.; Tang, T.; Ding, Y. F.; Zhang, Y. D.; Meng, F. Z., Synthesis and properties of SEPS-g-PEO copolymers with varying branch lengths. *Chin J Polym Sci* **2018,** *36*, 934-942.
29. Hong, B. B.; Panagiotopoulos, A. Z., Molecular dynamics simulations of silica nanoparticles grafted with poly(ethylene oxide) oligomer chains. *J Phys Chem B* **2012,** *116*, 2385−2395.
30. Grunewald, T. A.; Lassenberger, A.; van Oostrum, P. D. J.; Rennhofer, H.; Zirbs, R.; Capone, B.; Vonderhaid, I.; Amenitsch, H.; Lichtenegger, H. C.; Reimhult, E., Core-shell structure of monodisperse poly(ethylene glycol)-grafted iron oxide

nanoparticles studied by small-angle X-ray scattering. *Chem Mater* **2015,** *27*, 4763−4771.
31. Aranda, P.; Ruizhitzky, E., Poly(ethylene oxide)-silicate intercalation materials. *Chem Mater* **1992,** *4*, 1395−1403.
32. Rissanou, A. N.; Papananou, H.; Petrakis, V. S.; Doxastakis, M.; Andrikopoulos, K. S.; Voyiatzis, G. A.; Chrissopoulou, K.; Harmandaris, V.; Anastasiadis, S. H., Structural and conformational properties of poly(ethylene oxide)/silica nanocomposites: effect of confinement. *Macromolecules* **2017,** *50*, 6273−6284.
33. Chen, G. X.; Kim, H. S.; Park, B. H.; Yoon, J. S., Controlled functionalization of multiwalled carbon nanotubes with various molecular-weight poly(L-lactic acid). *J Phys Chem B* **2005,** *109*, 22237−22243.
34. Kato, K.; Uchida, E.; Kang, E. T.; Uyama, Y.; Ikada, Y., Polymer surface with graft chains. *Prog Polym Sci* **2003,** *28*, 209−259.
35. Stöber, W.; Fink, A., Controlled growth of monodisperse silica spheres in the micron size range. *J Colloid Interface Sci* **1968,** *26*, 62−69.
36. Shui, Y. D.; Su, Y. L.; Kuang, X.; Zhao, W. W.; Cai, Y. L.; Wang, D. J., Facile and controllable synthesis of hybrid silica nanoparticles densely grafted with poly(ethylene glycol). *Polym Int* **2017,** *66*, 1395−1401.
37. Zhao, W. W.; Su, Y. L.; Gao, X.; Xu, J. J.; Wang, D. J., Interfacial effect on confined crystallization of poly(ethylene oxide)/silica composites. *J Polym Sci Pt B-Polym Phys* **2016,** *54*, 414−423.
38. Lorenzo, A. T.; Arnal, M. L.; Albuerne, J.; Müller, A. J., DSC isothermal polymer crystallization kinetics measurements and the use of the Avrami equation to fit the data: Guidelines to avoid common problems. *Polym Test* **2007,** *26*, 222−231.
39. Galante, M. J.; Mandelkern, L.; Alamo, R. G.; Lehtinen, A.; Paukkeri, R., Crystallization kinetics of metallocene type polypropylenes - Influence of molecular weight and comparison with Ziegler-Natta type systems. *J Therm Anal* **1996,** *47*, 913−929.
40. Balsamo, V.; Urdaneta, N.; Perez, L.; Carrizales, P.; Abetz, V.; Müller, A. J., Effect of the polyethylene confinement and topology on its crystallisation within semicrystalline ABC triblock copolymers. *Eur Polym J* **2004,** *40*, 1033−1049.
41. Brandrup, J.; Immergut, E. H.; Grulke, E. A., Polymer Handbook. *New York: John Wiley & Sons* **1999**.
42. Fillon, B.; Wittmann, J. C.; Lotz, B.; Thierry, A., Self-nucleation and recrystallization of isotactic polypropylene (a phase) investigated by differential scanning calorimetry. *J Polym Sci Pt B-Polym Phys* **1993,** *31*, 1383−1393.
43. Michell, R. M.; Mugica, A.; Zubitur, M.; Müller, A. J., Self-Nucleation of crystalline phases within homopolymers, polymer blends, copolymers, and nanocomposites. *Adv Polym Sci* **2015,** *276*, 215−256.
44. Sunday, D.; Ilavsky, J.; Green, D. L., A Phase Diagram for Polymer-grafted nanoparticles in homopolymer matrices. *Macromolecules* **2012,** *45*, 4007−4011.
45. Akcora, P.; Liu, H.; Kumar, S. K.; Moll, J.; Li, Y.; Benicewicz, B. C.; Schadler, L. S.; Acehan, D.; Panagiotopoulos, A. Z.; Pryamitsyn, V.; Ganesan, V.; Ilavsky, J.; Thiyagarajan, P.; Colby, R. H.; Douglas, J. F., Anisotropic self-assembly of

spherical polymer-grafted nanoparticles. *Nat Mater* **2009,** *8*, 354−359.
46. Mangal, R.; Nath, P.; Tikekar, M.; Archer, L. A., Enthalpy-driven stabilization of dispersions of polymer-grafted nanoparticles in high-molecular-weight polymer melts. *Langmuir* **2016,** *32*, 10621−10631.
47. Wu, F.; Zhang, B.; Yang, W.; Liu, Z. Y.; Yang, M. B., Inorganic silica functionalized with PLLA chains via grafting methods to enhance the melt strength of PLLA/silica nanocomposites. *Polymer* **2014,** *55*, 5760−5772.
48. Müller, A. J.; Arnal, M. L.; Trujillo, M.; Lorenzo, A. T., Super-nucleation in nanocomposites and confinement effects on the crystallizable components within block copolymers, miktoarm star copolymers and nanocomposites. *Eur Polym J* **2011,** *47*, 614−629.
49. Müller, A. J.; Arnal, M. L., Thermal fractionation of polymers. *Prog Polym Sci* **2005,** *30*, 559−603.
50. Schmalz, H.; Müller, A. J.; Abetz, V., Crystallization in ABC triblock copolymers with two different crystalline end blocks: Influence of confinement on self-nucleation behavior. *Macromol Chem Physic* **2003,** *204*, 111−124.
51. Müller, A. J.; Balsamo, V.; Arnal, M. L.; Jakob, T.; Schmalz, H.; Abetz, V., Homogeneous nucleation and fractionated crystallization in block copolymers. *Macromolecules* **2002,** *35*, 3048−3058.
52. Balsamo, V.; Paolini, Y.; Ronca, G.; Müller, A. J., Crystallization of the polyethylene block in polystyrene-b-polyethylene-b-polycaprolactone triblock copolymers, 1 - Self-nucleation behavior. *Macromol Chem Physic* **2000,** *201*, 2711−2720.
53. Trujillo, M.; Arnal, M. L.; Müller, A. J.; Laredo, E.; Bredeau, S.; Bonduel, D.; Dubois, P., Thermal and morphological characterization of nanocomposites prepared by in-situ polymerization of high-density polyethylene on carbon nanotubes. *Macromolecules* **2007,** *40*, 6268−6276.
54. Córdova, M. E.; Lorenzo, A. T.; Müller, A. J.; Gani, L.; Tence-Girault, S.; Leibler, L., The influence of blend morphology (co-continuous or sub-micrometer droplets dispersions) on the nucleation and crystallization kinetics of double crystalline polyethylene/polyamide blends prepared by reactive extrusion. *Macromol Chem Physic* **2011,** *212*, 1335−1350.
55. Michell, R. M.; Blaszczyk-Lezak, I.; Mijangos, C.; Müller, A. J., Confinement effects on polymer crystallization: From droplets to alumina nanopores. *Polymer* **2013,** *54*, 4059−4077.
56. Loo, Y. L.; Register, R. A.; Ryan, A. J., Polymer crystallization in 25-nm spheres. *Phys Rev Lett* **2000,** *84*, 4120−4123.
57. Castillo, R. V.; Arnal, M. L.; Müller, A. J.; Hamley, I. W.; Castelletto, V.; Schmalz, H.; Abetz, V., Fractionated crystallization and fractionated melting of confined PEO microdomains in PB-b-PEO and PE-b-PEO diblock copolymers. *Macromolecules* **2008,** *41*, 879−889.
58. Carvalho, J. L.; Dalnoki-Veress, K., Homogeneous bulk, surface, and edge nucleation in crystalline nanodroplets. *Phys Rev Lett* **2010,** *105*.
59. Maiz, J.; Martin, J.; Mijangos, C., Confinement Effects on the Crystallization of

poly(ethylene oxide) nanotubes. *Langmuir* **2012,** *28*, 12296−12303.
60. Sabino, M. A.; Ronca, G.; Müller, A. J., Heterogeneous nucleation and self-nucleation of poly(p-dioxanone). *J Mater Sci* **2000,** *35*, 5071−5084.
61. Ding, J.; Maitra, P.; Wunder, S. L., Characterization of the interaction of poly(ethylene oxide) with nanosize fumed silica: Surface effects on crystallization. *J Polym Sci Pt B-Polym Phys* **2003,** *41*, 1978−1993.
62. Staszczuk, P.; Planda, M., The investigations of adsorption layers on material surfaces by means of the thermogravimetry technique. *Mater Chem Phys* **2001,** *70*, 305−315.
63. Fukuyama, Y.; Kawai, T.; Kuroda, S.; Toyonaga, M.; Taniike, T.; Terano, M., The effect of the addition of polypropylene grafted SiO2 nanoparticle on the crystallization behavior of isotactic polypropylene. *J Therm Anal Calorim* **2013,** *113*, 1511−1519.
64. Zdyrko, B. V., S. K.; Luzinov, I., Effect of molecular weight on synthesis and surface morphology of high-density poly(ethylene glycol) grafted layers. *Langmuir* **2004,** *20*, 6727−6735.
65. Zhao, W. W. S., Y. L.; Wen, X. N.; Wang, D. J., Manipulating crystallization behavior of poly(ethylene oxide) by functionalized nanoparticle inclusion. *Polymer*, *in press*, DOI: 10.1016/j.polymer.2019.01.019.
66. Zdyrko, B.; Klep, V.; Luzinov, I., Synthesis and surface morphology of high-density poly(ethylene glycol) grafted layers. *Langmuir* **2003,** *19*, 10179−10187.

For Table of Contents use only